Improved Double-Wall Artery High-Capacity Heat Pipe

R. Ponnappan*
Universal Energy Systems, Inc., Dayton, Ohio
and
Jerry E. Beam† and Tom Mahefkey‡
Air Force Wright Aeronautical Laboratories, Wright-Patterson Air Force Base, Dayton, Ohio

The double-wall artery heat pipe is a novel composite wick structure for high-capacity heat pipe designs. Encouraged by the initial test results (1600 W·m transport capacity and 16 W/cm^2 radial evaporator heat flux) of the proof-of-concept 1.2-m-long copper-water prototype, additional work has been performed to improve the transport capacity and overall performance of the double-wall heat pipe. The improved design reported in this paper incorporates a segmented grooved inner tube, larger arteries, and screenless adiabatic and condenser sections to allow longer transport length. Artery priming characteristics and performance test results of a 2-m-long, 2.22-cm-diam copper-water heat pipe unit are presented.

Nomenclature

g = acceleration due to gravity
w = artery groove width
ΔT = temperature difference
σ_l = liquid surface tension
ρ_l = liquid density
θ = wetting angle

Introduction

ADVANCED future space or terrestrial thermal systems require high-capacity heat pipes for the transport of thermal energy. The transport capacity of such heat pipes may be orders of magnitude higher than what current technology can provide. Newer designs to improve the heat-transfer and transport capabilities of heat pipes to meet futuristic requirements have been the major design goal for many heat pipe researchers. In this direction, one attempt to improve the present technology limitations, such as limited transport capacity, artery bubble blockage sensitivity, and low evaporator heat flux, has resulted in the development of what is called the "double-wall artery" high-capacity heat pipe.[1,2]

In this design, a slotted and externally grooved (axial grooves) inner tube wall, an inner-annuli screen mesh wick, and an outer envelope tube are packaged in a single concentric assembly. Several advantages of this composite wick geometry (such as separated vapor- and liquid-flow paths, high near-wall conductivity, better near-wall capillary pumping and fluid distribution, and radially subcooled artery with respect to heat addition at the evaporator wall) make this device attractive compared to other conventional composite-wick heat pipes. A nominal axial heat transport capacity of 1600 W·m and a radial heat flux density of 16 W/cm^2 were achieved under zero tilt conditions in the 1.2 m proof-of-concept prototype tests.[1,2] A unique behavior of decreasing evaporator ΔT with increasing heat input rate was observed and explained by a lean-wick evaporator countercurrent liquid/vapor flow model. This noted behavior of the double-wall arrangement evaporator is attributed to the subcooled artery grooves that supply liquid to the distributive screen wick radially outward, thereby reducing the possibilities of a film boiling crisis and consequent dry-out in the evaporator. In other words, the arteries of the double-wall design are protected from direct heating and remain separated from the vapor core. Other types of composite wicks (tunnel, pedestal, spiral, screen-over-groove, etc.) do not have these combined features.

Results of the 1.2 m heat pipe motivated further improvements and experimental investigation. This paper describes the design, fabrication, and testing of a 2-m-long improved double-wall artery heat pipe.

Design Description

The obvious choices for improvement of transport capacity were to increase the capillary pumping head and to reduce the liquid-flow friction loss. The capillary pumping head could be increased by increasing the screen mesh size (resulting in a smaller capillary pore radius and reduced permeability). Screen mesh size of $\sim 40 \times 40$ cm^{-1} used in previous models was adequate for a maximum pumping head up to 842 Pa at 127°C and hence the same mesh size was retained. Also, in view of the very good earlier evaporator performance, no configuration changes were made in the evaporator, except minor favorable dimensional changes such as increasing the evaporator length and artery depth and reducing the number of screen wraps from six to four. Two major modifications were introduced in the transport and condenser sections, as can be seen in Fig. 1. Namely, the transport artery cross-sectional flow area was increased and the screen in the transport and condenser sections was eliminated.

A major artery design change was to increase the artery groove size; the groove dimension was made three times larger (2.4 × 2.4 mm instead of 0.79 × 0.79 mm). The new size was derived from the optimistic design criterion requiring that the artery channel should self-prime according to the reduced Laplace-Young relation, wherein the priming height accounted for is the height of the artery groove,

$$w = \sqrt{2\sigma_l \cos\theta / \rho_l g} \tag{1}$$

It is assumed here that self-priming of each groove at the condenser would occur when the vapor condenses uniformly over the groove walls, irrespective of the different orientations of the grooves with respect to the gravity vector. In actuality, the groove pattern is symmetrical around the center. Therefore, it

Presented as Paper 84-1717 at the AIAA 19th Thermophysics Conference, Snowmass, CO., June 25-28, 1984; submitted July 2, 1984; revision submitted Sept. 25, 1984. This paper is declared a work of the U.S. Government and therefore is in the public domain.

*Thermal Systems Engineer, Research and Development Division. Member AIAA.
†Mechanical Engineer, Aerospace Power Division. Member AIAA.
‡Acting Chief, Energy Conversion Branch, Aerospace Power Division. Member AIAA.

is equally as possible that, while in the top groove gravity is a hindrance to heat pipe operation, the gravity may aid the heat transfer in the off-top locations by spreading the liquid to the screen at the evaporator.

The other major change incorporated was the total elimination of the screen wick in the transport and condenser sections, which eliminated the circumferential fluid communication and left each artery channel to prime independently. Incidentally, the possible uncertainty associated with the parallel screen/artery groove liquid-flow model assumed in the previous design was removed. The uncertainty concerned the relative amounts of axial liquid flow in the screen/groove composite. The screenless transport section provided a clear axial liquid transport model and eliminated cross flow between adjacent channels. It also provided more annular space for the artery groove.

The screenless condenser section reduced the effective thermal resistance and increased the metal-to-metal contact between the inner and outer tubes. Graded grooves (nonconstant groove widths for the evaporator, transport, and condenser sections) were employed in this design to minimize the transport pressure drop (by large adiabatic section grooves) and provide adequate evaporator distribution and condenser surface area (by small grooves). The graded groove design has been shown to reduce liquid-flow friction loss in the transport section and improve heat transfer in the condenser section.[3] Cross-sectional views of the three sections of the improved heat pipe are shown in Fig. 1.

As before, a copper-water system was chosen to demonstrate the proof-of-concept (screenless adiabatic) and to evaluate the performance of the improved design. Water has the advantages of a near-room temperature operating range (25-200°C), easy handling and processing, and compatibility with copper. A modified design approach based on standard design procedure applicable for a nonvariable conductance heat pipe was used (e.g., see Ref. 4). Standard available copper tubing that could withstand an internal pressure of 4.83 MPa (700 psi) at a maximum operating temperature of 250°C was chosen. The maximum pumping capacity corresponded to the capillary head of $\sim 40 \times 40\ \text{cm}^{-1}$ screen mesh, while the liquid pressure drop calculation was based on the dimensions of the new transport artery grooves. It was determined that the heat pipe transport capacity for this design was capillary limited in the working temperature range and the other operating limit factors were very high. A summary of design details is given in Table 1.

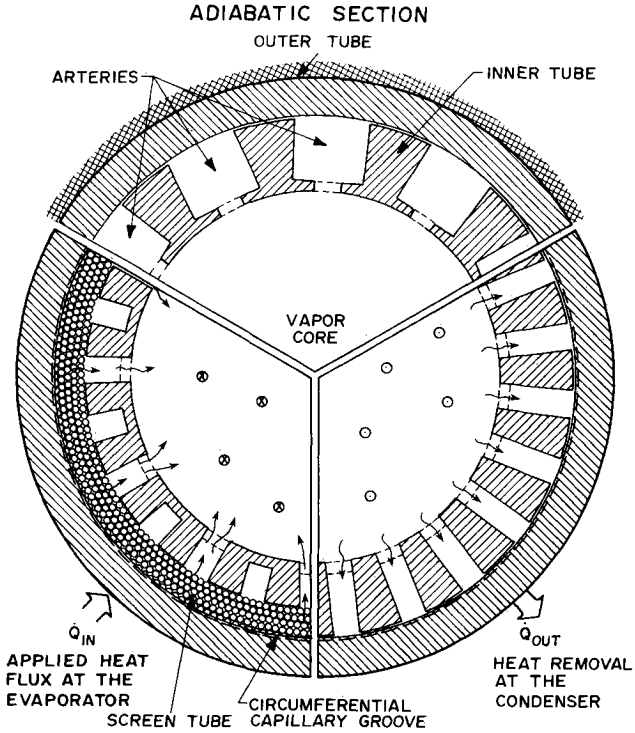

Fig. 1 Double-wall (modified) artery heat pipe wick configuration.

Artery Priming Considerations

In composite wicks, capillary pumping is achieved by small pores at the liquid/vapor interface. The most important requirement for a composite-wick heat pipe is that the smaller pore wick (screen) be sealed against the evaporated end. If this is not done, capillary pumping ability will be determined by the large gap or artery width.[5] In the present heat pipe, the evaporator end cap tightly sealed the end of the groove/screen composite. However, there were uncertainties about the priming phenomenon in double-wall artery heat pipe due to its unusual capillary geometry. It was one of the objectives of the present study to understand the priming characteristics of both the evaporator and condenser.

Two priming hypotheses are made. A desirable priming occurs when the liquid/vapor interface is maintained within the screen wick and liquid flows from the condenser grooves axially to the evaporator grooves via the transport grooves and then is capillary pumped radially outward to the screen. The other possibility of priming (which is a worst-case situation) occurs if the liquid/vapor interface recedes from the screen to the open evaporator groove; in such a situation, the capillary pumping is to be determined by the evaporator artery groove width. The capillary head will be very much lower in the latter case. The expected capillary limits calculated for both cases are plotted in Fig. 2.

In the absence of the circumferential liquid distribution at the condenser section (screenless), it is necessary to have uniform vapor condensation over the walls of the condenser grooves. Hence, uniform external heat removal is important. However, due to the effect of gravity (in 1 g testing), liquid puddling at the bottom of the condenser may be inevitable. If this happens, the arteries at the top may not prime full and could cause premature evaporator dry-out. In order to overcome this problem, a special operating procedure has to be introduced as described in the section on experimental procedure.

Fabrication and Experiments

Fabrication

The 2.22 cm o.d. outer tube was made of type K hard copper tubing and the inner tube was machined from 1.89 cm o.d., 3 mm thick wall OFHC copper tubing. The evaporator

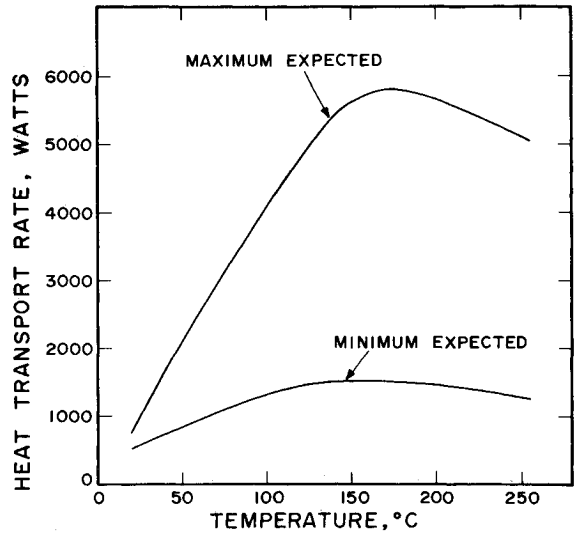

Fig. 2 Theoretical capillary transport capacity limit.

Table 1 Modified double-wall heat pipe design summary

Material			
Outer tube, evaporator end cap and fill tube	Copper (Type K hard drawn)		
Inner tube and condenser flow swirler	Copper (OFHC)		
Condenser end-cap	Copper (OFHC)		
Fill valve	Brass body with Kel-F seat		
Wick	Copper screen mesh		
Working fluid	Water		
Overall details			
Temperature range	25-250°C		
Heat transport capacity (Capillary limited)	6473 W·m at 100°C		
Effective length	1.575 m		
Total length	2.03 m		
Evaporator length	0.305 m		
Adiabatic length	1.115 m		
Condenser length	0.610 m		
Vapor core diameter	1.27×10^{-2} m		
Overall diameter	2.22×10^{-2} m		
Wick			
Type	Double-wall artery wick featuring nonconstant groove widths and screenless adiabatic & condenser sections		
Screen size (evaporator)	$\sim40\times40$ cm^{-1}		
Number of spiral wraps	4		
Artery grooves	Evaporator	Transport	Condenser
No.	24	12	24
Width, mm	0.79	2.38	0.79
Depth, mm	1.4	2.38	2.38
Vapor vents			
No. per groove	24 on alternate grooves	117 on all grooves	42 on all grooves
Size, mm	6×0.79	3×0.79	12.7×0.79
Axial spacing between slots, mm	6	6	1.5
Heat transport limit (horizontal mode of operation)			
Maximum capillary pumping head	849.9 Pa at 127°C		
Maximum available pumping head	667.6 Pa at 127°C		
Liquid pressure drop in artery channels	0.0581 Pa per W·m at 127°C		
Vapor pressure drop in vapor core	0.0243 Pa per W·m at 127°C		
Capillary transport limitation (controlling limit for this design)	5142 W at 127°C		
Fluid inventory			
Quality	Demineralized, deionized water (18 MΩ·cm resistance)		
Quantity	130.4 cm^3 filled at room temperature		

portion of the inner tube was recessed to accomodate four layers of $\sim40\times40$ cm^{-1} screen and the transport and condenser portions were slip fitted within the outer tube. The inner side of the outer tube was machined to form 40 threads/cm fine-circumferential V-threads in the evaporation length. The inner tube was grooved using precision saw-cutter and slotted using ELOX electro-discharge machining. The groove and vapor vent arrangement and dimensions are given in Fig. 3. The inner tube was not machined in one piece due to its long length (2 m). It was made of three short sections of one 30 cm long evaporator piece and two equal pieces of the remaining length. The matching ends of each section were suitably notched to align the grooves. All of the parts were thoroughly vapor degreased and chemically cleaned in accordance with standard procedures before assembly. The end caps were TIG (tungsten/inert gas) welded in an argon-circulated glove box.

The heat pipe was pumped down to a pressure $\sim10^{-6}$ mm Hg (Torr) and baked at 180°C for 8 h, then filled with 130 cm^3 of water in a heat pipe filling rig through the fill valve welded to the condenser end cap.

Experimental Procedure

The schematic diagram of the experimental setup is shown in Fig 4. The evaporator section was heated by a wrapped resistance heating coil contact, while the condenser section was cooled by water-drip evaporative cooling. On the heat pipe wall, 21 externally mounted copper-constantan thermocouples monitored the temperatures and performance of the heat pipe. The transport and evaporator lengths were insulated with 5-10 cm thick Fiberfrax§ insulation. The a.c. electric power input to the heaters was measured by means of a wattmeter. The overall loss of energy through the insulation, mounting brackets, etc., was assumed to be less than 12% of the input power as determined from previous calorimetric measurements. The heat pipe was aligned on the mounting brackets to assure horizontal conditions. Four leveling screws on the mounting base permitted adverse or favorable tilt settings as desired. Only steady-state tests were conducted by ap-

§Fiberfrax is a registered trademark of the Carborundum Company.

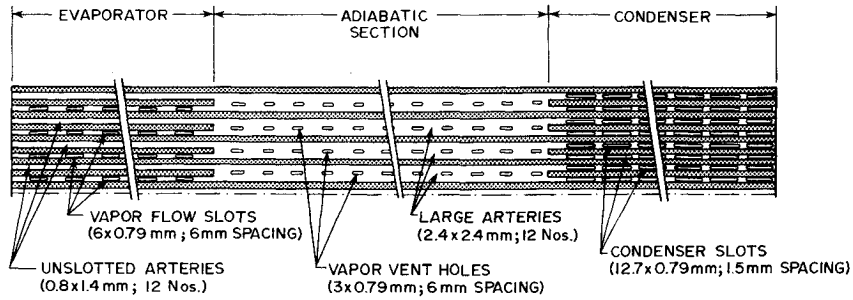

Fig. 3 Groove and vapor vent details of the inner tube.

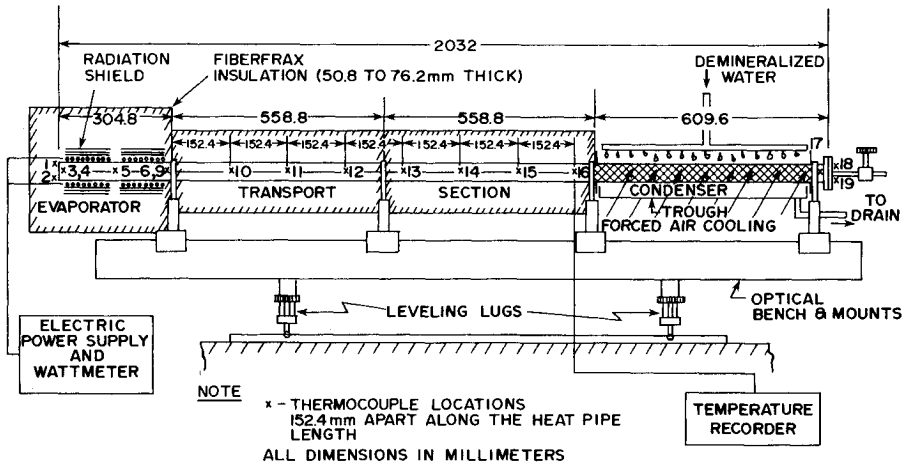

Fig. 4 Heat pipe (2 m) test setup schematic.

plying constant power input to the heater and observing the steady-state temperature of the heat pipe. The evaporator and condenser ΔT computed from the measured steady-state axial wall temperatures and the average adiabatic section temperature were recorded as measures of the heat pipe performance.

In order to eliminate the quenching effect created by the direct water-drip evaporative cooling at the condenser section, an external thermal resistance was included in the heat-transfer path. A split cylinder stainless steel collar called the "heat choke" (241 mm long and 9.5 mm thick) was tightly fitted over the condenser and one layer of screen wrapped over this collar. This arrangement was tried subsequent to the normal method. The addition of the collar raised the operating temperature of the heat pipe by 22°C typically at 750 W and decreased the quenching problem of the condenser. The increased temperature also shifted the performance of the heat pipe toward the peak operating point and resulted in an increased transport capacity of 1225 W (see Fig. 5).

An additional important procedure followed in testing this heat pipe was to raise the entire heat pipe to a higher temperature level than the expected steady-state temperature by applying low-power input to the evaporator for a long period of time, while not force cooling the condenser. Then, the power input was increased in large steps (500 W) while the drip cooling was also started. Essentially, a steady-state condition by the cool-down mode was obtained, as opposed to the traditional heating method. In this manner, the experimental transport maximum attained was larger than that by the traditional method of steady state by the heating mode.

Results and Discussions

Figure 5 shows the axial temperature variation of the heat pipe. Only 30 cm of the 60 cm condenser length was used, since the full-length condenser created an overquenching effect that led to condenser flooding and consequent evaporator dry-out. Initially, power inputs larger than 500 W could not be transported with 60 cm condenser cooling. On the other hand, with only a 30 cm condenser at the fill tube end, 800 W was transported without the heat choke and 1225 W with the heat choke. The vapor pressure recovery phenomenon marked by the lower temperature at the middle of the condenser, as noted in Fig. 5, could be the reason for the condenser flooding. It may be recalled that the thermal resistance of this heat pipe had been reduced compared to the 1.2 m heat pipe. It was also observed that combined forced-air convection cooling with the water drip produced additional overcooling of condenser and led to premature evaporator dry-out. Hence, mostly water-drip natural convection evaporative cooling was used. Improved condenser performance for low input power is obvious from the low temperature difference (ΔT) between the adiabatic and condenser sections for this 2 m heat pipe compared to a large ΔT (on the order of 10-50°C) in the 1.2 m heat pipe. This is due to the elimination of screen wick in the condenser, which reduced the internal thermal resistance.

Another important observation made during this as well as previous unit testing is that the heat pipe's overall performance with respect to evaporator ΔT and transport capacity improved with the increasing number of hours of testing until a stage when noncondensible gas generation began. This improvement in performance with time may be attributed to the increase in the wettability of the internal surface, which is known to change with time. As the testing (burn-in) progressed, the heat pipe seasoned better and the wettability became more uniform. Figure 6 shows this evaporator temperature difference improvement with cumulative testing.

The predicted maximum transport capacity of this heat pipe has not been obtained with the present test conditions. However, a transport of 2100 W·m has been demonstrated at an average pipe temperature of 166°C with a 1225 W input and 1.72 m effective length. This is about 30% more than the 1.2 m heat pipe design that transport 1600 W·m at 200°C. Difficulties are faced in selecting an appropriate condenser cooling rate. Improper external conditions are thought to influence the "wet point" (where $P_v = P_1$) and the consequent internal pressure recovery. Acoustically observed forced internal flow oscillations caused premature evaporator dry-out. In the present setup, the condenser cooling rate can be varied

only arbitrarily. Instead, a well-instrumented calorimetric-type cooling system has to be used to preselect a desired cooling rate that will match the input power. Also, it is necessary that the average condenser temperature should match that of the heat pipe in order to avoid any condenser quenching effects. This may be accomplished with oil bath cooling or gas-gap calorimetry.

Apparently, the heat pipe does not exhibit any priming problem, due either to the large-sized arteries or to the elimination of screen wick in the condenser and transport sections. Every time a dry-out occurred, the power input was reduced or removed and the evaporator was found to reprime with the liquid. In order to rule out the possibility of any puddle flow augmenting the priming of wick, adverse tilt tests were conducted and it was ascertained that the arteries primed by themselves. Typically, at an adverse tilt of 0.3 deg (with the evaporator end 1 cm higher than the condenser end), the transport was 1000 W. Figure 7 shows the tilt test results. At level testing, however, with power inputs higher than 1300 W, a crisis developed at the evaporator and caused dry-out. Efforts are under way to derive the expected maximum performance of this heat pipe.

The theoretical capillary transport limit based on the evaporator groove as the pumping wick has been compared with the experimental data in Fig. 8. It can be seen in this figure that the transport capacity has improved with the heat choke installed on the condenser. Also, it is noticed that the heat pipe operated at relatively lower temperatures with longer condenser lengths. For example, the average adiabatic temperature was 90°C with a 60 cm condenser and 110°C with a 30 cm condenser for a 500 W input (Figs. 5 and 8).

As a result of the less than optimal performance, the overall design approach has been reviewed. The basic concept behind the improved design is to decrease the friction loss of the fluid flow in the long transport section, while maintaining the large capillary pressure generated by the small pores in the screen of the evaporator section. This concept has been used before and has been reported to have a much larger heat transport capacity than the conventionally designed grooved heat pipes.[3] As discussed earlier, a concern was raised about whether the screen in the evaporator section would remain the primary pumping wick or if the screen would deprime and require the groove to provide for the pumping of the liquid. Figure 9 exemplifies this concern showing a possible model for the evaporator dry-out and priming mechanism for a single groove. It can be noticed in Fig. 9c that the screen is completely dried out and the liquid/vapor interface has receded into the groove and that at this heat input the evaporator priming depends on the groove width. Therefore, it is a concern what capillary structure actually drives the fluid flow. The results suggest that the area of composite-wick pumping capability is far from being understood and warrants some ad-

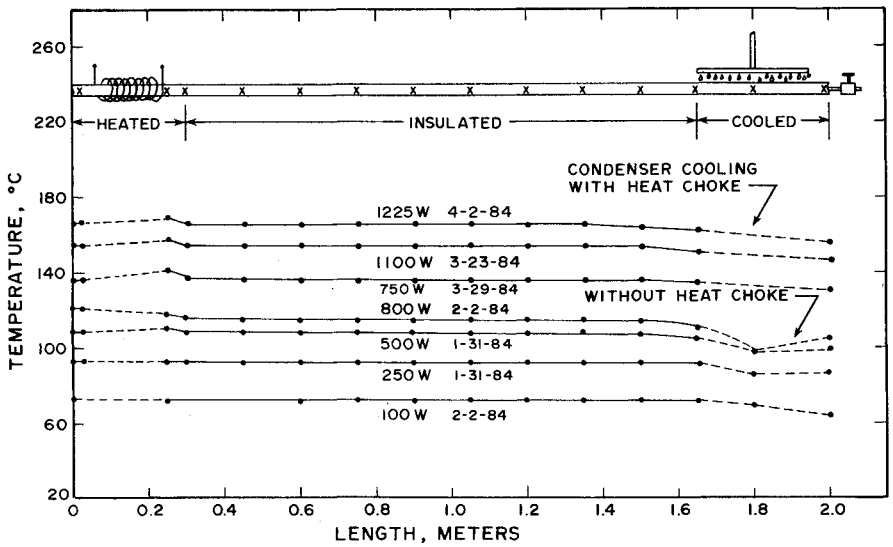

Fig. 5 Axial temperature distribution (level test).

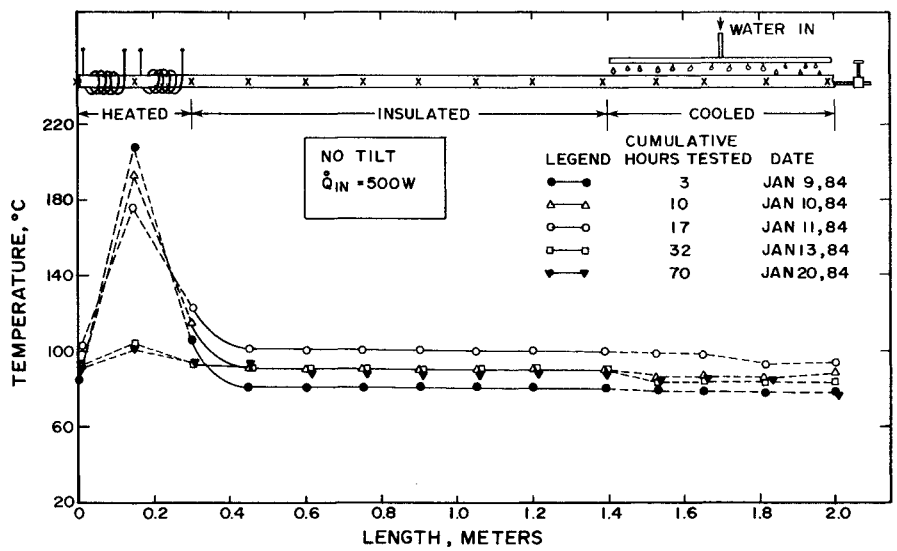

Fig. 6 Evaporator temperature variation with testing.

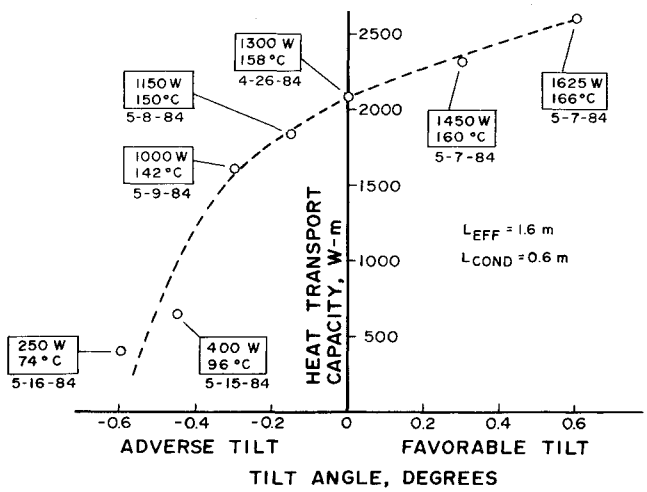

Fig. 7 Heat transport capacity vs tilt angle.

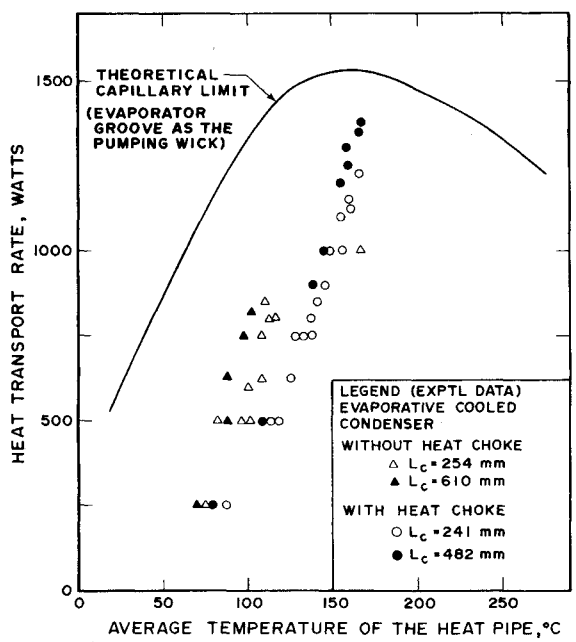

Fig. 8 Heat transport rate vs temperature.

ditional investigation. In addition, the results suggest the possibility of a capillary pumping problem with the current design that was not apparent in the previous design.[1,2]

Conclusions

A 2 m long modified version of the double-wall artery heat pipe has been designed and fabricated. The test results show that the average operating temperature and the overall ΔT have been lowered considerably compared to the 1.2 m heat pipe. The maximum transport capacity attained is 2100 W·m, which is 30% more than that of the 1.2 m heat pipe.

The improved performance is due to the threefold increase in the size of the artery channels. However, the optimistic design limit of 6473 W·m could not be attained at this stage. The possible problem areas such as the uncertainties of the wick wetting conditions and the governing capillary pump mechanism call for further investigation.

The screenless condenser operated with a ΔT of ~7°C at a power input of 1225 W as opposed to a ΔT of more than 25°C

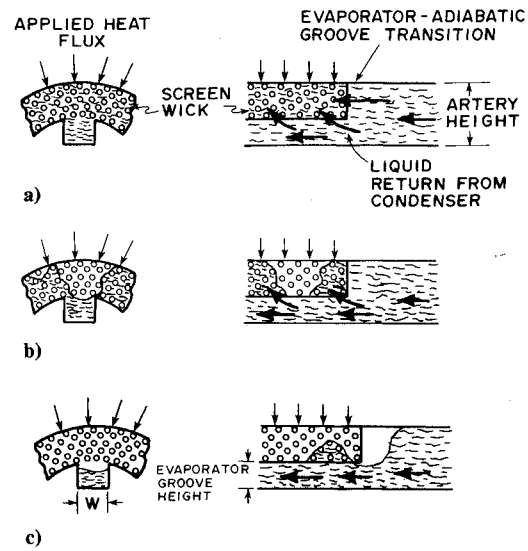

Fig. 9 Evaporator dry-out and priming mechanism: a) fully saturated screen and groove; b) liquid-vapor interface recedes into the groove; c) screen completely dried out—evaporator priming depends on the groove width.

in the previous condenser design having six layers of screen. The stainless steel heat choke mounted on the condenser raised the operating temperature of the heat pipe by 22°C, as expected, and helped to maximize the transport capacity. This device evidently decreased the condenser quenching problem and the acoustically observed flow oscillations inside the heat pipe.

The improved design demonstrates the working of a composite wick in which the capillary pumping and the transport liquid-flow friction effects are decoupled. The removal of the screen wick in the adiabatic length has not adversely affected the priming characteristics of the heat pipe, while this flexibility helps to build double-wall heat pipes with very large transport lengths. However, the exact mechanism of priming of the double-wall arrangement evaporator from the screenless large-sized adiabatic artery channels needs to be studied.

Acknowledgments

The work described in this paper was conducted at the Air Force Wright Aeronautical Laboratories under the sponsorship of the Air Force Office of Scientific Research. Technical help provided by Charles Hall (AFWAL) and John Tennant (UES) for this project is sincerely acknowledged.

References

[1]Ponnappan, R. and Mahefkey, T., "Development of a Double-Wall Artery High-Capacity Heat Pipe," *AIAA Progrss in Astronautics and Aeronautics*: *Spacecraft Thermal Control, Design, and Operation,* Vol. 86, edited by H.E. Collicott and P.E. Bauer, AIAA, New York, 1983, pp. 202-221.

[2]Ponnappan R. and Mahefkey, T., "Performance Characteristics of the Double-Wall Artery High Capacity Heat Pipe," AIAA Paper 83-0318, Jan. 1983.

[3]Schlitt, K.R., "Development of an Axially Grooved Heat Pipe with Non-Constant Groove Widths," AIAA Paper 78-375, May 1978.

[4]Chi, S.W., *Heat Pipe Theory and Practice,* McGraw-Hill Book Co., New York, 1976.

[5]Wright, J.P., "Computer Program for the Design and Analysis of Heat Pipes," North American Rockwell Space Division, Downey, CA, Rept. SD-72-SA-0001, Jan. 1972.